RESEARCH ARTICLE | APRIL 13 2018

New evaluation parameter for wearable thermoelectric generators ⊘

Dimuthu Wijethunge (ID) ; Woochul Kim
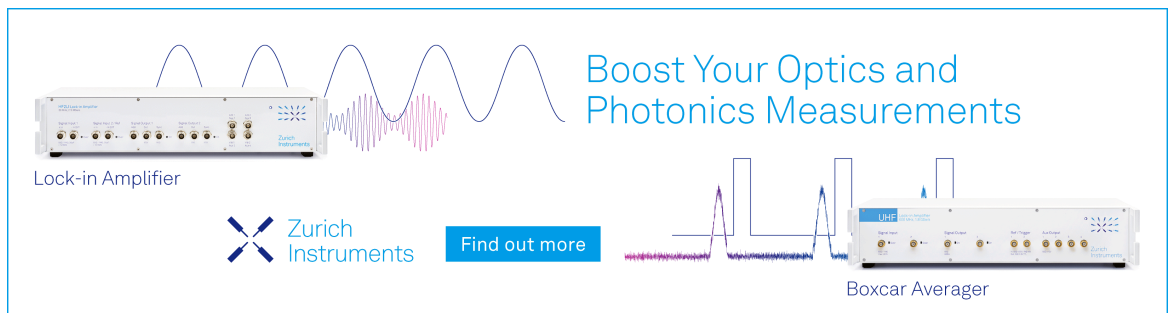
Check for updates

View Online

Export Citation

New evaluation parameter for wearable thermoelectric generators

Dimuthu Wijethunge and Woochul Kim[a)]
School of Mechanical Engineering, Yonsei University, Seoul 120-749, South Korea

Wearable devices constitute a key application area for thermoelectric devices. However, owing to new constraints in wearable applications, a few conventional device optimization techniques are not appropriate and material evaluation parameters, such as figure of merit (zT) and power factor (PF), tend to be inadequate. We illustrated the incompleteness of zT and PF by performing simulations and considering different thermoelectric materials. The results indicate a weak correlation between device performance and zT and PF. In this study, we propose a new evaluation parameter, $zT_{wearable}$, which is better suited for wearable applications compared to conventional zT. Owing to size restrictions, gap filler based device optimization is extremely critical in wearable devices. With respect to the occasions in which gap fillers are used, expressions for power, effective thermal conductivity (k_{eff}), and optimum load electrical ratio (m_{opt}) are derived. According to the new parameters, the thermal conductivity of the material has become much more critical now. The proposed new evaluation parameter, namely, $zT_{wearable}$, is extremely useful in the selection of an appropriate thermoelectric material among various candidates prior to the commencement of the actual design process. *Published by AIP Publishing.* https://doi.org/10.1063/1.5018762

I. INTRODUCTION

Following the discovery of thermoelectric concepts in the 18th century, thermoelectric devices to date do not perform at a satisfactory level. The nonexistence of efficient natural thermoelectric materials and inverse proportionality between thermoelectric properties, i.e., Seebeck coefficient, S, thermal conductivity, k, and electrical conductivity, σ, are the major causes for the performance lag in thermoelectric devices. Owing to the nanostructured material design approach,[1,2] the performance of thermoelectric devices is increasing at a significant pace. Thus, the thermoelectric figure of merit, zT, and power factor, PF, which are defined below, are considered as the main evaluation parameters for thermoelectric materials[3]

$$zT = \frac{S^2 \sigma}{k} T, \qquad (1)$$

$$PF = S^2 \sigma. \qquad (2)$$

Equation (3) expresses the conventional relationship between the material zT and maximum thermal efficiency, η_{max},[4,5] and thereby illustrates the main reason for using zT as a material evaluation parameter. According to Eq. (3), the energy conversion efficiency of the material increases with zT. Hence, extensive studies mainly focused on the development of materials with peak zT, and recent state-of-the-art bulk thermoelectric materials exhibit maximum zT in the range of 2–2.6.[1,6] In Eq. (3), the temperatures on the hot and cold sides are denoted by T_h and T_c, respectively,

$$\eta_{max} = \frac{\Delta T}{T_h} \frac{\sqrt{zT+1}-1}{\sqrt{zT+1}+\frac{T_c}{T_h}}. \qquad (3)$$

Similarly, the power factor (PF) is another parameter that illustrates the extractable power output of the material for a given temperature difference. However, with respect to certain applications, such as wearable thermoelectrics, both the conventional evaluation parameters tend to be quite unreasonable. This issue is explored in a few studies related to wearable thermoelectric devices.[7,8] However, a proper explanation of this issue is largely absent. With respect to high-temperature applications, the insufficiency of zT is clearly highlighted by Kim *et al.*[9,10] Both parameters, zT and PF, are appropriate as evaluation parameters when the temperature of both the hot and the cold sides is constant and independent of the material properties, and when the temperature difference between the hot and cold sides is small so that temperature dependency of material properties is less important. If the application displays a high temperature difference, a modified version of zT termed as "ZT_{eng}" was proposed by Kim *et al.*[9,10] to more accurately solve the temperature dependency of material properties. In wearable devices, the temperature difference across the thermoelectric elements is insignificant owing to high skin thermal resistance, high skin to device thermal contact resistance, and high heat sink thermal resistance[11–13] compared to those of the thermoelectric device. Therefore, conventional zT and PF may not be appropriate for estimating device performance. Therefore, in the present study, we propose a considerably improved parameter termed as "$zT_{wearable}$" for wearable devices.

Thermoelectric element height and area are key optimizable parameters in conventional thermoelectric devices although this optimization technique is considerably impractical for wearable devices owing to size limitations. With respect to devices with non-optimized leg height, gap fillers are important in terms of power output. Thus, the device

---

a)E-mail: woochul@yonsei.ac.kr

optimization scheme for wearable devices is different from those of conventional devices. Therefore, the present study involves proposing an appropriate device optimization scheme for wearable thermoelectric devices. Furthermore, a few thermoelectric materials were investigated, and the results indicate that certain materials with low *PF* and *zT* exhibit increased potential exceeding those of the materials with higher *PF* and *zT* in terms of power output for use in wearable applications.

II. THEORETICAL ANALYSIS

A. Module without the gap filling material

The analytical solution for thermoelectric devices is obtained by simply solving the two energy balance equations that are constructed by considering the incoming (Q_{in}) and outgoing (Q_{out}) heat flows at the two ends of the thermoelectric element. The construction of the equations is based on the resistance network illustrated in Fig. 1(a). The thermal resistances of hot and cold sides are indicated as R_{hot} and R_{cold}, respectively. The temperatures of hot and cold sides of the device are given by T_{hot} and T_{cold}, respectively, and T_h and T_c correspond to the hot and cold side temperatures of the thermoelectric element such that ΔT is the difference in temperatures of the hot and cold sides, i.e., $\Delta T = T_h - T_c$. The Thomson effect is generally negligible for applications
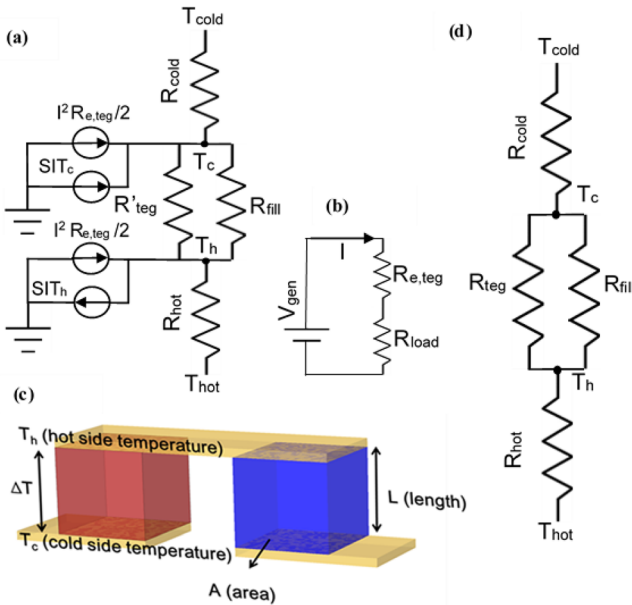
with low temperature difference and also for materials with a constant Seebeck coefficient. Thus, the Thomson effect is not considered in the calculations. The expressions are as follows:

$$Q_{in} = \frac{T_{hot} - T_h}{R_{hot}} = kA\frac{\Delta T}{L} + SIT_h - \frac{1}{2}I^2 R_{e,teg}, \quad (4)$$

$$Q_{out} = \frac{T_c - T_{cold}}{R_{cold}} = kA\frac{\Delta T}{L} + SIT_h - \frac{1}{2}I^2 R_{e,teg}. \quad (5)$$

Here, the height and area of the thermoelectric element are given by L and A, respectively. Additionally, I and $R_{e,teg}$ denote the current and electrical resistance of the element, respectively.

With respect to wearable thermoelectric devices, it is further simplified by neglecting the Joule heating term owing to its minor contribution to the temperature profile given the low current and electrical resistance. Neglecting the Joule heating term can be a reasonable approximation as shown in Fig. 2 which is an example when the maximum power output is around $6\,\mu$W/cm^2. Subsequently, Peltier and conduction heat transfer are represented as effective thermal conductivity terms. Baranowski et al.[14] derived the expression for effective thermal conductivity, k_{eff}, for thermoelectric generators, and Apertet et al.[15] then improved this for closed circuit conditions. The expression for effective thermal conductivity is given in Eq. (6). The ratio of load electrical resistance to internal electrical resistance is given by $m = R_{e,load}/R_{e,teg}$ as follows:

$$k_{eff} = k\left(1 + \frac{zT_h}{1+m}\right). \quad (6)$$

By this approach, the Peltier effect can be treated as an increase in the thermal conductivity of the material, although
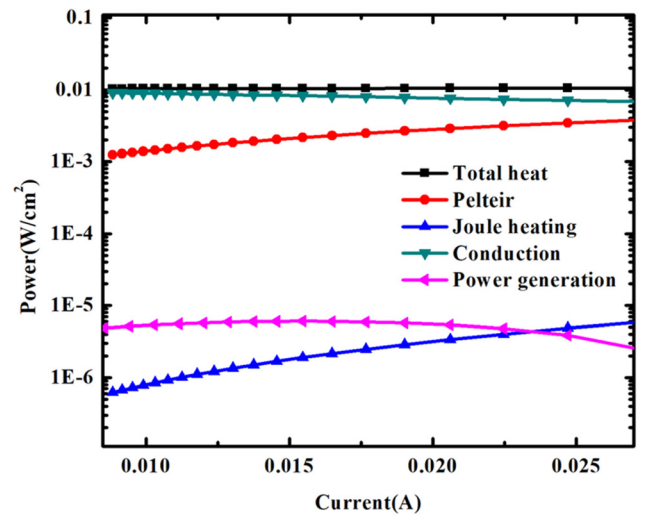

FIG. 1. (a) Equivalent thermal resistance network for the wearable thermoelectric device including hot side temperature (T_{hot}), hot side external thermal resistance (R_{hot}), hot side temperature of the thermoelectric element (T_h), filler material thermal resistance (R_{fill}), thermoelectric element thermal resistance (R'_{teg}), cold side temperature (T_{cold}), cold side external thermal resistance (R_{cold}), and cold side temperature of the thermoelectric element (T_c). (a) Peltier effect is indicated by the term SIT and joule heating at each end is given by I^{2}R$_{e,teg}$/2. (b) Equivalent electrical resistance network for the wearable thermoelectric device, internal electrical resistance of the thermoelectric device ($R_{e,teg}$), generated voltage of the thermoelectric device (V_{teg}), load electrical resistance ($R_{e,load}$), and voltage across load resistance (V_{load}). (c) Schematic of the thermoelectric device. (d) Simplified version of the equivalent thermal resistance network which was obtained neglecting joule heating and including the Peltier term into thermoelectric element resistance (R_{teg}).

FIG. 2. Total heat flow, Q_{in}, and components comprising the heat flow relative to the electrical load resistance, $R_{e,load}$. Here, the change in load resistance is represented by the corresponding electrical current. The total heat (body heat) comprises the heat transferred through conduction, the Peltier effect, and the Joule heating effect. The simulation conditions and parameters [R$_{hot}$ = 0.04 m^2 K/W, R$_{cold}$ = 0.1 m^2 K/W, T$_{cold}$ = 20 °C, T$_{hot}$ = 36 °C, S = 232 μV/K, σ = 70 000 S/m, k = 0.7 W/m K, and fill factor (FF) = 0.2] are selected to represent the wearable thermoelectric device.

the Peltier effect occurs at the interface. So, the thermal resistance of the device can be expressed as given in Eq. (7). Then, the thermal resistance network in Fig. 1(a) can be simplified as in Fig. 2(d)

$$R_{teg} = \frac{L}{Ak_{eff}}. \tag{7}$$

Based on this reasoning, i.e., neglecting Joule heating and including Peltier heat flow into the thermal conduction, the relationship between temperatures and thermal resistances can be obtained as follows:

$$Q_{in} = \frac{T_h - T_c}{R_{teg}} = \frac{T_{hot} - T_{cold}}{R_{teg} + R_{hot} + R_{cold}}. \tag{8}$$

When deducing Eq. (8), Q_{in} is assumed to be equal to Q_{out} so that heat flux is constant throughout the device. In wearable thermoelectric generators, the device efficiency is very low due to the small temperature difference between the human body and atmosphere. For example, according to Eq. (3), the maximum obtainable device efficiency is at most 3.34% for a body temperature of 310 K and an ambient temperature of 273 K and for a material with a zT of 2, which is an overestimated example. Therefore, it is reasonable to assume Q_{in} is comparable to Q_{out} for wearable applications

$$T_h - T_c = \frac{T_{hot} - T_{cold}}{1 + \frac{R_{hot} + R_{cold}}{R_{teg}}} = \frac{T_{hot} - T_{cold}}{1 + \frac{AK_{eff}(R_{hot} + R_{cold})}{L}}, \tag{9}$$

$$P = \frac{V_{load}^2}{R_{e,load}} = \frac{V_{teg}^2}{R_{e,load}} \left(\frac{m}{m+1}\right)^2 = \frac{S^2(T_h - T_c)^2}{R_{e,load}} \left(\frac{m}{m+1}\right)^2, \tag{10}$$

$$R_{e,load} = mR_{e,teg} = m\frac{L}{\sigma A}. \tag{11}$$

Combining Eqs. (9)–(11), we derive the simple expression for power output, P, which is given in Eq. (12). The term R_{ext}'' is expressed as $A(R_{hot} + R_{cold})$ as follows:

$$P = \frac{L\sigma AS^2(T_{hot} - T_{cold})^2}{R_{ext}''^2 \left(\frac{L}{R_{ext}''^2} + k_{eff}\right)^2} \frac{m}{(m+1)^2}. \tag{12}$$

To calculate power output, the zT_h term needs to be known. For wearable devices, it is reasonable to assume that T_h is close to the skin temperature. Additionally, the material property zT is not sensitive to smaller changes in temperature. Therefore, material zT values closer to the skin temperature can be used to solve the equations. In this work, material properties such as zT, S, k, and σ around a temperature of 300 K are used for the calculations.

The maximum power occurs when $dP/dm = 0$. Thus, the optimum electrical resistance ratio, m_{opt}, which satisfies the condition is given as follows:

$$m_{opt} = 1 + \frac{kzT_h}{\frac{L}{R_{ext}''} + k}. \tag{13}$$

Similarly, thermal efficiency and the corresponding optimum load ratio, m_{opt}, for maximum thermal efficiency, are expressed in Eqs. (15) and (16). The detailed derivation is given in the supplementary material (SI 1–SI 5)

$$\eta \equiv \frac{P}{Q_{in}} = \frac{S^2\sigma(T_h - T_c)}{k_{eff}} \frac{m}{(m+1)^2}, \tag{14}$$

$$\eta = \frac{LS^2\sigma(T_{hot} - T_{cold})}{k_{eff}R_{ext}'' \left(\frac{L}{R_{ext}''} + k_{eff}\right)} \frac{m}{(m+1)^2}. \tag{15}$$

Maximum efficiency occurs when $d\eta/dm = 0$. Thus, the optimum electrical resistance ratio, m_{opt}, which satisfies the condition is given as follows:

$$m_{opt} = \sqrt{(1 + zT_h)} \sqrt{\frac{(1 + zT_h)k + \frac{L}{R_{ext}''}}{\frac{L}{R_{ext}''} + k}}. \tag{16}$$

In situations where $L/R_{ext}'' \ll k_{eff}$, the external thermal resistance per unit area exceeding the internal thermal resistance per unit area R_{int}' can be shown by the following expression:

$$\frac{L}{R_{ext}''} \ll k_{eff}$$
$$R_{ext}'' \gg \frac{L}{k_{eff}} \approx R_{int}''. \tag{17}$$

Subsequently, power and efficiency are proportional to the material properties as given in Eqs. (18) and (19). The corresponding optimum m_{opt} for both cases is given in Eq. (20) as follows:

$$P \propto \frac{S^2\sigma}{k_{eff}^2} \frac{m}{(m+1)^2}, \tag{18}$$

$$\eta \propto \frac{S^2\sigma}{k_{eff}^2} \frac{m}{(m+1)^2}, \tag{19}$$

$$m_{opt} = 1 + zT_h. \tag{20}$$

In this case, the importance of the power factor, $PF = S^2\sigma$, divided by the effective thermal conductivity, k_{eff}, with respect to the second power is clearly observed. However, when $R_{ext}'' \ll R_{int}''$, i.e., internal thermal resistance per unit area is very much larger than the external thermal resistance per unit area, power output and efficiency are proportional to the material properties as given in the following equations:

$$P \propto S^2\sigma \frac{m}{(m+1)^2}, \tag{21}$$

$$\eta \propto \frac{S^2\sigma}{k_{eff}} \frac{m}{(m+1)^2}. \tag{22}$$

Thus, conventional material evaluation parameters (zT, PF) are not effective, especially in cases where high external thermal resistance per unit area is presented compared with

the internal thermal resistance per unit area. However, when the internal thermal resistance is very much larger than the external resistances,the   conventional evaluation parameter *PF* becomes sufficient to evaluate the material's power generation capability as indicated by Eq. (21). Therefore, the evaluation parameter should be changed accordingly while developing materials for wearable applications.

To maximize the power output, internal thermal resistance can be optimized which is known as thermal load matching in thermoelectric generators. Internal thermal resistance can be changed by adjusting the thermoelectric leg height. Yazawa and Shakouri[16] derived an equation to obtain optimum leg height, L_{opt}, which maximizes the power output in thermoelectric generators. For the symmetric hot and cold side thermal resistances, the optimum leg height can be calculated using the following equation:[16]

$$L_{opt} = m\,k\,R''_{ext}, \quad m = \sqrt{1+zT}. \tag{23}$$

In practice, thermoelectric element heights cannot reach an optimum value due to manufacturing and practical constrains in wearable applications. Usually, external thermal resistances are high as 0.14 m^2 K/W for wearable devices, so that L_{opt} becomes also high making it impractical to use elements with such heights. Therefore, best practice would be to consider the highest possible element height.

B. Module with the gap filling material

In wearable devices, the main functions of gap fillers are to increase the flexibility and structural stability of the device. Proper choice of the gap filler material reduces heat loss through air convection since the filler material can inhibit bulk air flow and also restrict the heat conduction through the device. When the thermal conductivity of the gap filler materials is lower than the thermoelectric material, then the temperature difference across the element can be increased by using gap filler materials. Simultaneously, it also restricts occupiable space for thermoelectric elements which results in increase in the internal electrical resistance of the device. Therefore, the power output can be increased by using gap fillers only if the correct proportion is used. Eom et al.[17] used an acyl based filler to construct a flexible structure for the wearable thermoelectric generator. Kim et al.[18,19] used a polymer based filler material with a low thermal conductivity of 0.03 W/m K to increase the power output of the wearable thermoelectric generator. Suarez et al.[7] used air as the filler material in the non-flexible wearable thermoelectric generator to increase the power output and later designed a flexible version of the generator using polydimethylsiloxane (PDMS) as the gap filling material.[20] Park et al.[21] used a mat like structure constructed by a polymer and wires to develop a flexible thermoelectric cooling device. Lu et al.[22] used fabric filler materials to construct a thermoelectric generator for wearable applications.

The fill factor is the ratio between the thermoelectric element area, A, and total area, A$_{total}$, which is expressed as follows:

$$FF = \frac{A}{A_{total}}. \tag{24}$$

Thus, the effective thermal conductivity is expressed as given in Eq. (25), where k_f denotes the thermal conductivity of the filler material.

$$k_{eff} = k\left[FF + \frac{k_f}{k}\cdot(1-FF) + \frac{zT_h}{1+m}\cdot FF\right]. \tag{25}$$

Similarly, the power equation is updated by considering the filler material as follows:

$$P = \frac{L\sigma A_{total}\,FF\,S^2(T_{hot} - T_{cold})^2}{R''^2_{ext,FF}\left(\dfrac{L}{R''_{ext,FF}} + k_{eff}\right)^2}\frac{m}{(m+1)^2}. \tag{26}$$

Thus, m_{opt}, that yields the maximum power, is given as shown in the following equation:

$$m_{opt} = 1 + \frac{kzT_h.FF}{\dfrac{L}{R''_{ext,FF}} + k.FF + k_f.(1-FF)}. \tag{27}$$

Derivation of Eqs. (25), (26), and (27) is given in the supplementary material (SI 6–SI 8). When the external thermal resistance exceeds the internal thermal resistance, the expression is as follows:

$$\frac{L}{R''_{ext,FF}} \ll k_{eff},$$
$$R''_{ext,FF} \gg \frac{L}{k_{eff}} \approx R''_{int}. \tag{28}$$

Thus, power is proportional to material properties as given in the following equation:

$$P \propto \frac{FF.S^2\sigma}{k^2_{eff}}\frac{m}{(m+1)^2}. \tag{29}$$

Hence, irrespective of the existence of a filler material, the power output is proportional to the power factor, $PF = S^2\sigma$, divided by the effective thermal conductivity, k_{eff}, to the second power for a given fill factor.

C. Optimum fill factor

In most occasions, the minimum and maximum fill factors are fixed owing to manufacturing limitations. It is observed that the optimum fill factor changes with respect to the thermoelectric material properties and also with respect to element height. Therefore, it is important to obtain the optimum *FF* in advance to ensure a better evaluation of materials. Several simulations in which *FF* is varied are performed, and an accurate optimum value is easily calculated. Although this method is time consuming, the derivation of a simple expression for optimum *FF* is a considerably difficult task mainly because *m* is dependent on the fill factor. The average value for *m* is assumed, and the accurate approximation is performed for the optimum filler factor that is only

TABLE I. Various material properties and optimum fill factor calculations for device conditions used for the simulation in Fig. 3.

Material	k (W/m K)	σ (S/m)	S (μV/K)	zT	PF (V/K)	$zT_{wearable}$ (FF = 100%)	Optimum FF Eq. (31)	$zT_{wearable}$ (FF = optimum)
$Bi_{0.5}Sb_{1.5}Te_3$ Nanostructured	0.7	70 000	232	1.61	0.0037	1.01	27	1.29
PEDOT:PSS[23]	0.31	90 000	70	0.42	0.0004	0.82	153	0.88
Cu_2Se[24]	0.62	25 000	200	0.48	0.001	0.49	45	0.56
$Bi_{0.5}Sb_{1.5}Te_3/Bi_2Te_{2.7}Se_{0.3}$ bulk	1	61 000	215	0.84	0.0028	0.47	21	0.75
Bi_2Te_3/Sb_2Te_3 superlattice[25]	1.15	85 515	257	1.48	0.0056	0.6	15	1.09
Holey silicon[26]	1.73	30 000	250	0.32	0.0018	0.14	14	0.32
$Bi_{0.3}Sb_{1.7}Te_3/Bi_2Te_{2.7}Se_{0.3}$ Screen printed[19]	0.84	68 600	184	0.83	0.0023	0.55	26	0.77

used for estimation purposes. According to Eq. (27), the maximum value of m is $zT + 1$ and the minimum value for m is 1. Thus, the average value for m, m_{avg}, is considered in the following equation:

$$m_{avg} = 1 + \frac{zT}{2}, \quad (30)$$

$$FF_{opt} = \frac{\dfrac{L}{A_{total}(R_{hot} + R_{cold})} + k_f}{k - k_f + \dfrac{kzT_h}{1 + m}}. \quad (31)$$

Using Eq. (31), the optimum fill factor is approximated with acceptable accuracy. Derivation of the equation is given in the supplementary material section (SI 9).

III. RESULTS AND DISCUSSION

We analyzed typical wearable thermoelectric generator devices with variable geometrical parameters and materials. The thermoelectric properties of the representative cases are listed in Table I, and they were used for the graphs in Fig. 3. Simulations were performed for a fixed thermoelectric element height of 5 mm, $R_{hot} = 0.04$ m^2 K/W, $R_{cold} = 0.1$ m^2 K/W, $T_{cold} = 20\,^\circ$C, and $T_{hot} = 36\,^\circ$C. The thermal conductivity of the gap filler material is 0.21 W/m K. As shown in Fig. 3,
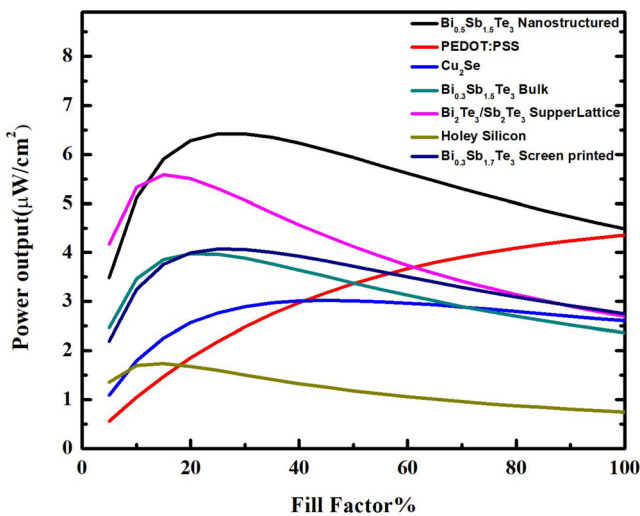

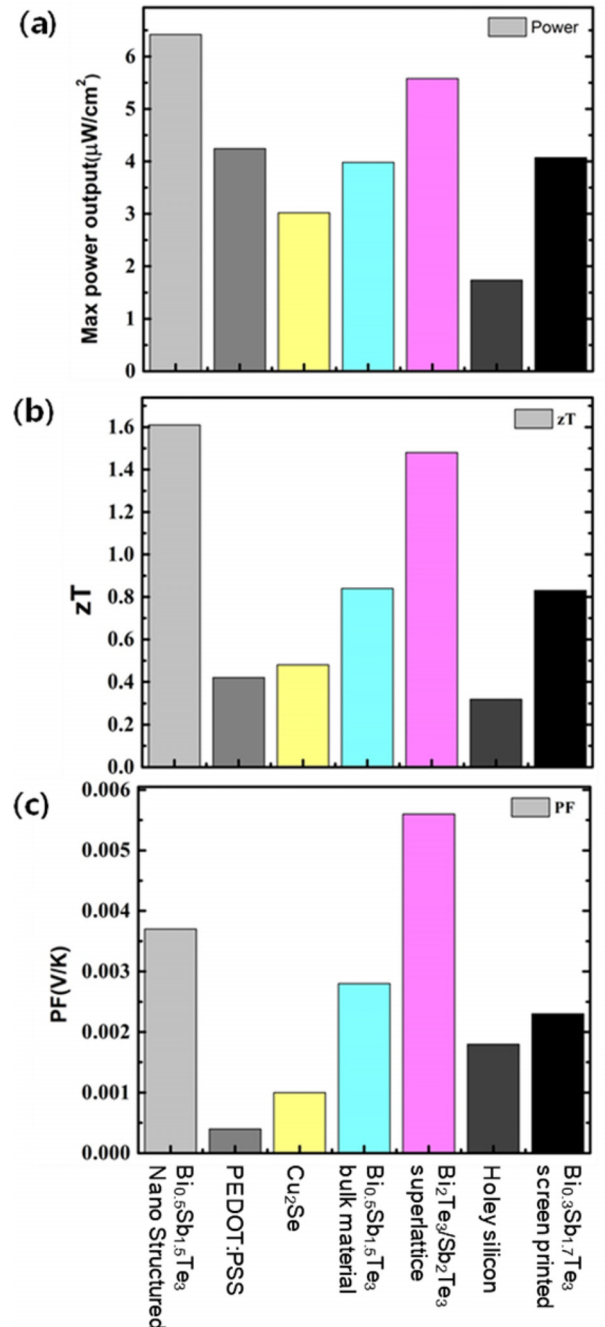FIG. 3. Power output relative to fill factors for different thermoelectric material properties (see Table I).

FIG. 4. (a) Maximum power output for any fill factor for the given conditions, (b) the thermoelectric figure of merit, zT, and (c) the power factor (PF) of various thermoelectric materials.

when the fill factor is considered to be 100%, i.e., no filler material, the highest power output is obtained in the nano-structured $Bi_{0.5}Sb_{1.5}Te_3$ and PEDOT:PSS materials. Based on the material properties shown in Table I, PEDOT:PSS exhibits the lowest power factor and moderate zT although it produces power that is almost equal to its counterpart, namely nano-structured $Bi_{0.5}Sb_{1.5}Te_3$ with the zT of 1.61. This is a good example in which conventional material evaluation parameters such as zT and PF are insufficient.

When the filler material is used, most of the materials exhibited increased performance with the exception of PEDOT: PSS. As shown in Fig. 4(a), the highest maximum power is observed in the nanostructured $Bi_{0.5}Sb_{1.5}Te_3$ that exhibits the highest zT followed by the material with the second highest zT, i.e., the Bi_2Te_3/Sb_2Te_3 superlattice. Given the power factor, the Bi_2Te_3/Sb_2Te_3 superlattice exhibits the highest power factor among the materials listed although its output power is lower than that of the nanostructured $Bi_{0.5}Sb_{1.5}Te_3$, which exhibits a lower power factor. The next highest power output is displayed by PEDOT:PSS that exhibits a lower zT and power factor compared to a few of the remaining materials (Cu_2Se, $Bi_{0.5}Sb_{1.5}Te_3$ and $Bi_2Te_{2.7}Se_{0.3}$, and screen printed

$Bi_{0.3}Sb_{1.7}Te_3/Bi_2Se_{0.3}Te_{2.7}$). The main reason for the enhanced power output corresponds to the inclusion of filler materials with lower thermal conductivity. This reduces the effective thermal conductivity as shown in Eq. (25).

Figure 5 shows variation of the device power output with temperature differences between the hot and cold side for seven different materials which were the same as used in Fig. 3. Figure 5(a) shows the power output for an arbitrary fixed fill factor value of 0.5 while Fig. 5(b) shows the maximum power output obtainable for any fill factor. In Fig. 5, R_{hot}, R_{cold}, and L are taken as 0.04 m^2 K/W, 0.1 m^2 K/W, and 0.005 m, respectively. Differences between the hot and cold side temperatures are varied from 1 °C to 36 °C. Generally, in wearable applications, the body temperature remains constant while the ambient temperature varies. So, here, a maximum temperature difference of 36 °C is observable when the ambient temperature is 0 °C and material properties assumed to be constant throughout the temperature range. Figures 5(c) and 5(d) show the zT and PF values of respective materials.

From both graphs, no correlation between the power output to zT and PF. In the fixed fill factor graph,
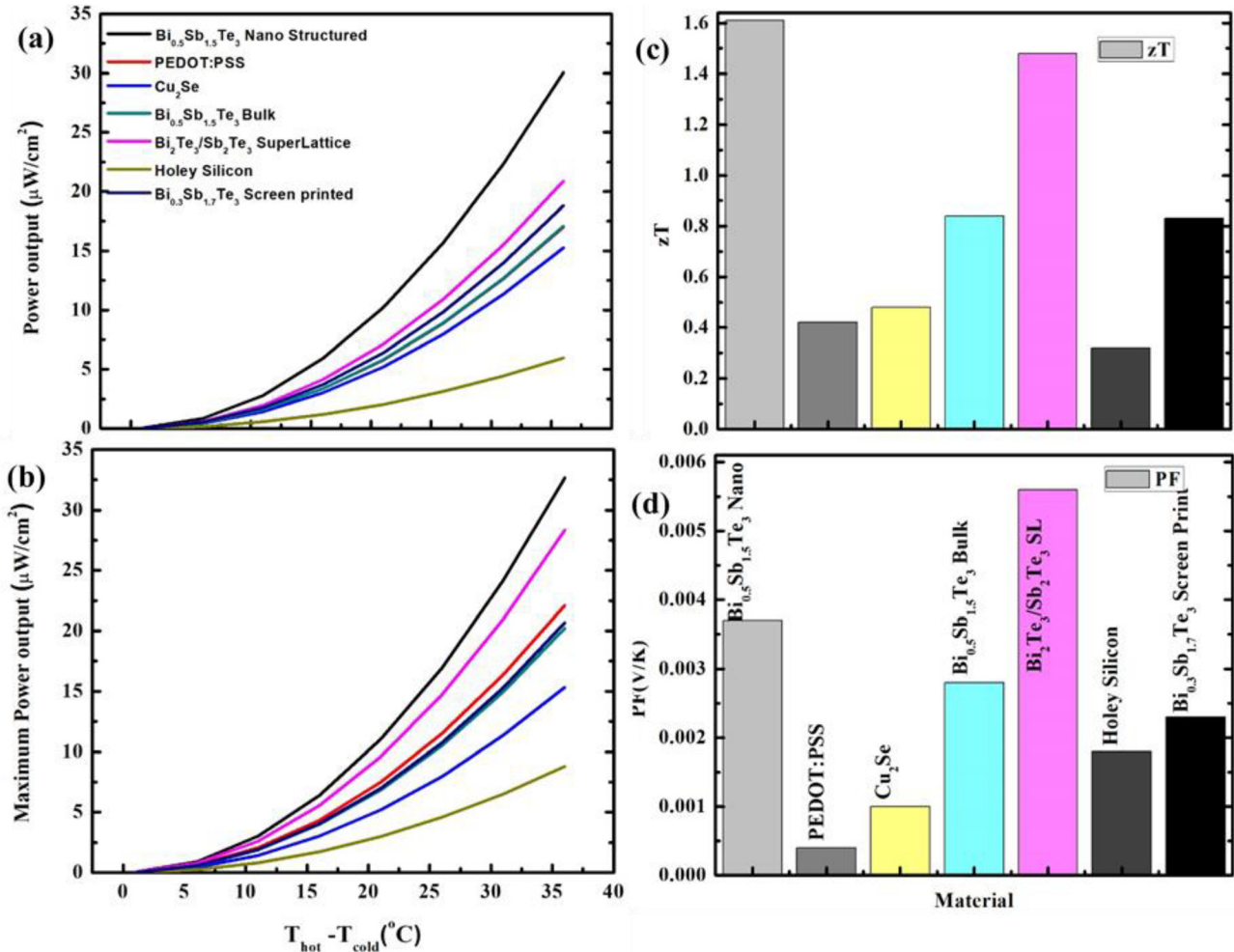

FIG. 5. (a) Power output with respect to hot (T_{hot}) and cold (T_{cold}) side temperature difference for an arbitrary fill factor of 0.5 and different thermoelectric materials. (b) Maximum power output with respect to hot (T_{hot}) and cold (T_{cold}) side temperature difference for any fill factor and different thermoelectric materials. The device conditions considered include $R_{hot} = 0.04$ m^2 K/W, $R_{cold} = 0.1$ m^2 K/W, and L = 0.005 m. (c) The thermoelectric figure of merit, zT, and (d) the power factor (PF) of various thermoelectric materials.

PEDOT:PSS shows similar power to the $Bi_{0.5}Sb_{1.5}Te_3$/$Bi_2Te_{2.7}Se_{0.3}$ bulk material and the $Bi_{0.3}Sb_{1.7}Te_3$ screen printed material showing higher power output than the $Bi_{0.5}Sb_{1.5}Te_3$/$Bi_2Te_{2.7}Se_{0.3}$ bulk material. In the maximum power output graph, PEDOT:PSS exhibits higher power output than Cu_2Se, $Bi_{0.5}Sb_{1.5}Te_3$/$Bi_2Te_{2.7}Se_{0.3}$, and screen printed $Bi_{0.3}Sb_{1.7}Te_3$/$Bi_2Se_{0.3}Te_{2.7}$ materials which have higher zT and PF compared to PEDOT:PSS. These graphs also highlight the importance of having a fill factor term in the evaluation parameter. For example, if the device should have a fill factor of 0.5 due to external reasons, then it can be shown that the $Bi_{0.3}Sb_{1.7}Te_3$ screen printed material is more suitable than PEDOT:PSS. However, if there is no restriction, PEDOT:PSS would be a better choice over the $Bi_{0.3}Sb_{1.7}Te_3$ screen printed material as it gives the maximum power output. Additionally, all materials show obvious increase in power output with respect to the increasing temperature difference between the hot and cold sides.

Figures 6(a) and 6(b) show the power output versus element height for a fixed fill factor value of 0.5 and maximum obtainable power put for any fill factor versus element height, respectively. Also, Figs. 6(c) and 6(d) present the zTs and PFs of materials used in the simulation. Element height ranges from 1 mm to 19 mm while R_{hot}, R_{cold}, T_{hot}, and T_{cold} have constant values of 0.04 m^2 K/W, 0.1 m^2 K/W, 36 °C, and 20 °C, respectively. Similar to previous results, the maximum power output keeps increasing with the element heights, but the rate of increment decreases suggesting that the power output only increases for up to a certain leg height. Although the power output in the fixed fill factor shows relationship with zTs and PFs values, especially in element heights around 8 to 19 mm, when the maximum power output is considered, the correlation with the power output to conventional evaluation parameters, i.e., zTs and PFs, does not exist as PEDOT:PSS exhibits higher power output than Cu_2Se throughout the range and almost equal power to $Bi_{0.5}Sb_{1.5}Te_3$/$Bi_2Te_{2.7}Se_{0.3}$, and screen printed $Bi_{0.3}Sb_{1.7}Te_3$/$Bi_2Se_{0.3}Te_{2.7}$ which are much higher zT and PF materials.

By considering all aspects, here we introduce a new term referred to as $zT_{wearable}$ to evaluate materials for applications based on its power generating ability. It should be noted that $zT_{wearable}$ is not dimensionless in contrast to the thermoelectric figure of merit, zT. It is expressed in Eq. (32). With respect to the derivation of new zT, the
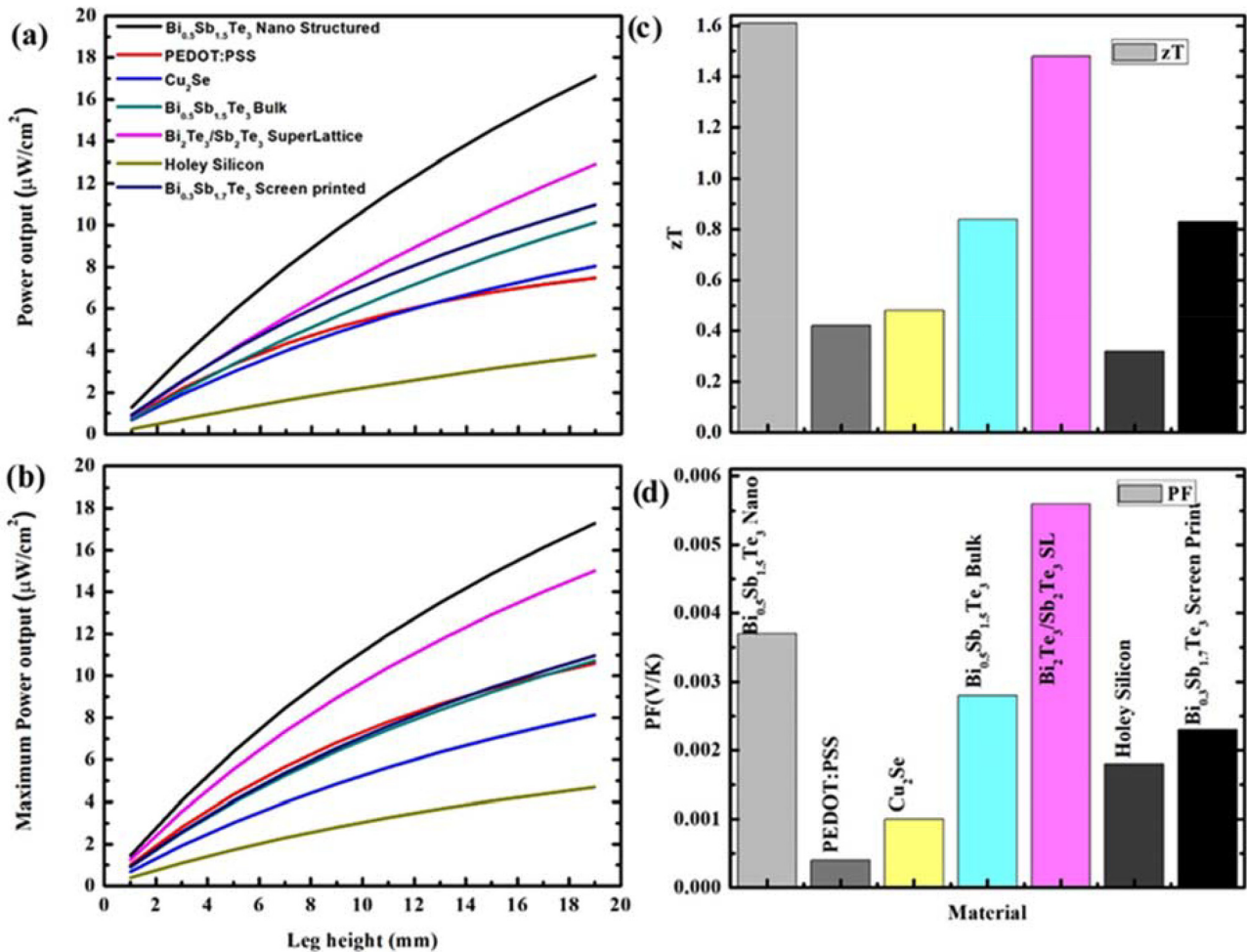

FIG. 6. (a) Power output with respect to thermoelectric element height (L) for an arbitrary fill factor of 0.5 and different thermoelectric materials. (b) Maximum power output with respect to element height for any fill factor and different thermoelectric materials. The simulation conditions and parameters ($R_{hot} = 0.04$ m^2 K/W, $R_{cold} = 0.1$ m^2 K/W, $T_{cold} = 20$ °C, and $T_{hot} = 36$ °C). (c) The thermoelectric figure of merit, zT, and (d) the power factor (PF) of various thermoelectric materials.
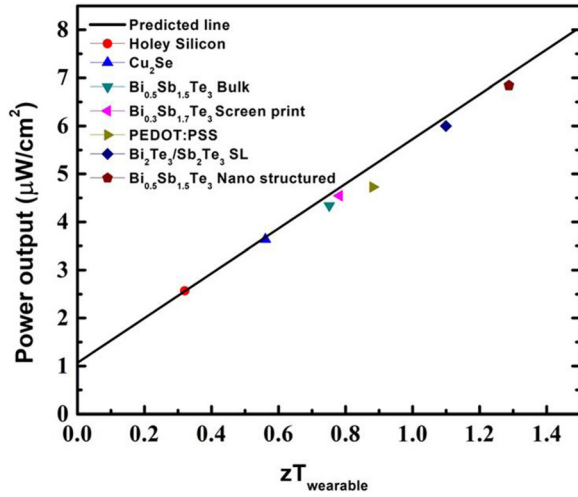
FIG. 7. Variation in device power output relative to the $zT_{wearable}$ parameter in a line graph. The device conditions considered include $R_{hot} = 0.04$ m^2 K/W, $R_{cold} = 0.1$ m^2 K/W, $T_{cold} = 20\,°$C, $T_{hot} = 36\,°$C, and $L = 0.005$ m. Corresponding power output obtained by using different materials when optimum fill factor % (see Fig. 3) is given by the points.

contribution of the term $m/(1 + m)^2$ is assumed as independent of material properties although this term is slightly dependent on the material properties. Given a material with zT corresponding to 1, the maximum value for term $[m/(1 + m)^2]$ is 0.25 (when $m = 1$) and the minimum value is 0.22 (when $m = 2$).

$$zT_{wearable} = FF_{opt} \frac{S^2\sigma}{\left(\dfrac{L}{R''_{ext,FF}} + k_{eff}\right)^2} T$$

$$k_{eff} \gg \frac{L}{R''_{ext,FF}}; \quad zT_{wearable} = FF_{opt} \frac{S^2\sigma}{k_{eff}^2} T$$

$$k_{eff} \ll \frac{L}{R''_{ext,FF}}; \quad zT_{wearable} = FF_{opt} \frac{S^2\sigma}{\left(\dfrac{L}{R''_{ext,FF}}\right)^2} T.$$

(32)

Figure 7 illustrates the power generation capability relative to $zT_{wearable}$ for certain conditions. As shown in the graph, the power output varies linearly with the parameter. As clearly shown in Fig. 7, the proposed parameter $zT_{wearable}$ provides accurate power output estimation in wearable thermoelectrics. In the graph plot, m is considered as 2, although it changes slightly with material properties and external conditions values, and this is the reason for the slight deviation between material power output values and line graph. Here, the fill factor is based on the optimum value for each case. Thus, according to the $zT_{wearable}$ values, the material with the highest power output is clearly distinguishable irrespective of whether a filler is used.

IV. CONCLUSION

The main parameters that are used to evaluate thermoelectric performance include conventional evaluation

parameters such as the thermoelectric figure of merit, zT, and the power factor, PF. However, the aforementioned parameters are not adequate for a few applications and especially for applications involving wearable thermoelectric devices. In this study, the inadequacy of these parameters is explained by using theoretical equations and through simulations. We presented a more suitable thermoelectric evaluation parameter termed as $zT_{wearable}$ for wearable thermoelectric devices. The effectiveness of this expression relative to the existing evaluation parameters is discussed by using simulations based on various representative materials. The new parameter indicates that the thermal conductivity of the material has become more critical now. Therefore, low thermally conductive materials, such as polymer based thermoelectric materials, display additional advantages over inorganic thermoelectric materials. Thus, the use of polymer based materials is encouraged in thermoelectric wearable devices. The proposed new evaluation parameter, namely $zT_{wearable}$, is extremely useful in the selection of appropriate thermoelectric materials with respect to various candidates prior to the commencement of the actual design process.

SUPPLEMENTARY MATERIAL

See supplementary material for detailed derivations of the equations for effective thermal conductivity (k_{eff}), output power (P), efficiency (η), optimum load ratio (m_{opt}), and optimum fill factor (FF_{opt}).

ACKNOWLEDGMENTS

[1]H. Wang, J.-H. Bahk, C. Kang, J. Hwang, K. Kim, J. Kim, P. Burke, J. E. Bowers, A. C. Gossard, A. Shakouri, and W. Kim, Proc. Natl. Acad. Sci. U.S.A. **111**, 10949 (2014).
[2]S. I. Kim, K. H. Lee, H. A. Mun, H. S. Kim, S. W. Hwang, J. W. Roh, D. J. Yang, W. H. Shin, X. S. Li, Y. H. Lee, G. J. Snyder, and S. W. Kim, Science **348**, 109 (2015).
[3]H. J. Goldsmid, *Introduction to Thermoelectricity* (Springer, Berlin, Heidelberg, 2010), p. 7.
[4]A. F. Ioffe, L. Stil'bans, E. Iordanishvili, T. Stavitskaya, A. Gelbtuch, and G. Vineyard, Phys. Today **12**(5), 42 (1959).
[5]E. Altenkirch, Physik. Zeits **10**, 560 (1909).
[6]L.-D. Zhao, S.-H. Lo, Y. Zhang, H. Sun, G. Tan, C. Uher, C. Wolverton, V. P. Dravid, and M. G. Kanatzidis, Nature **508**, 373 (2014).
[7]F. Suarez, A. Nozariasbmarz, D. Vashaee, and M. C. Ozturk, Energy Environ. Sci. **9**, 2099 (2016).
[8]M. T. Dunham, M. T. Barako, S. LeBlanc, M. Asheghi, B. Chen, and K. E. Goodson, Energy **93**, 2006 (2015).
[9]H. S. Kim, W. Liu, G. Chen, C.-W. Chu, and Z. Ren, Proc. Natl. Acad. Sci. U.S.A. **112**, 8205 (2015).
[10]H. S. Kim, W. Liu, and Z. Ren, Energy Environ. Sci. **10**, 69 (2017).
[11]D. Wijethunge, D. Kim, and W. Kim, J. Phys. D: Appl. Phys. **51**, 055401 (2018).
[12]J.-H. Bahk, H. Fang, K. Yazawa, and A. Shakouri, J. Mater. Chem. C **3**, 10362 (2015).
[13]K. Pietrzyk, J. Soares, B. Ohara, and H. Lee, Appl. Energy **183**, 218 (2016).
[14]L. L. Baranowski, G. J. Snyder, and E. S. Toberer, J. Appl. Phys. **113**, 204904 (2013).
[15]Y. Apertet, H. Ouerdane, C. Goupil, and P. Lecoeur, J. Appl. Phys. **115**, 126101 (2014).

[16]K. Yazawa and A. Shakouri, J. Appl. Phys. **111**, 024509 (2012).

[17]Y. Eom, D. Wijethunge, H. Park, S. H. Park, and W. Kim, Appl. Energy **206**, 649 (2017).

[18]C. S. Kim, G. S. Lee, H. Choi, Y. J. Kim, H. M. Yang, S. H. Lim, S.-G. Lee, and B. J. Cho, Appl. Energy **214**, 131 (2018).

[19]S. J. Kim, H. E. Lee, H. Choi, Y. Kim, J. H. We, J. S. Shin, K. J. Lee, and B. J. Cho, ACS Nano **10**, 10851 (2016).

[20]F. Suarez, D. P. Parekh, C. Ladd, D. Vashaee, M. D. Dickey, and M. C. Öztürk, Appl. Energy **202**, 736 (2017).

[21]H. Park, D. Kim, Y. Eom, D. Wijethunge, J. Hwang, H. Kim, and W. Kim, J. Phys. D: Appl. Phys. **50**, 494006 (2017).

[22]Z. Lu, H. Zhang, C. Mao, and C. M. Li, Appl. Energy **164**, 57 (2016).

[23]G. H. Kim, L. Shao, K. Zhang, and K. P. Pipe, Nat. Mater. **12**, 719 (2013).

[24]B. Yu, W. Liu, S. Chen, H. Wang, H. Wang, G. Chen, and Z. Ren, Nano Energy **1**, 472 (2012).

[25]G. E. A. Bulman, Nat. Commun **7**, 10302 (2016).

[26]J. Tang, H.-T. Wang, D. H. Lee, M. Fardy, Z. Huo, T. P. Russell, and P. Yang, Nano Lett. **10**, 4279 (2010).